Ultraviolet photodetector characteristics of ZnO-CuO nanofiber heterostructures

Roonak Abdul Salam A.Alkareem[1], Raad S. Sabry[2]

Department of physics, college of science, Mustansiriyah University, Baghdad, Iraq

roonak_1988@uomustansiriyah.edu.iq

Abstract

In this work, zinc oxide (ZnO) nanofibers fabricated by electrospinning technique and ZnO-CuO nanofiber heterostructures UV photodetector by combining electrospinning and dip coating methods. The prepared samples were characterized by X-ray diffraction (XRD), field emission scanning electron (FESEM), and UV-visible.

ZnO nanofiber and ZnO-CuO nanofiber heterostructures showed high selectivity in 350 nm and 410 nm, respectively. Also, the samples showed high responsivity, detectivity, and efficiency under low bias voltage and also low power density. The current-voltage (I-V) characteristics were determined under different wavelength from mercury lamp.

Keywords: Zinc Oxide, Nanofibers, heterostructures, photodetector.

وصف الالياف النانوية المهجنة لاوكسيد الخارصين-اوكسيد النحاس ككاشف ضوئي للأشعة فوق البنفسجية

م.م. روناك عبدالسلام عبدالكريم ، أ.د. رعد سعدون صبري

الجامعة المستنصرية/ كلية العلوم/ قسم الفيزياء

الخلاصـــة:

في هذا العمل، تم تكوين الياف نانوية لأوكسيد الخارصين بطريقة البرم الكهربائي و الياف نانوية مهجنة لأوكسيد الخارصين – اوكسيد النحاس ككاشف ضوئي للأشعة فوق البنفسجية بأستخدام دمج

طريقتي البرم الكهربائي و التغطيس. تم وصف العينات المتكونة باستخدام حيود الاشعة السينية (XRD)، مسح المجهر الانبعاث الالكتروني (FESEM) والفحوصات البصرية.

ان الالياف النانوية لأوكسيد الخارصين و الالياف المهجنة لأوكسيد الخارصين-اوكسيد النحاس بين انتقائية عالية عند الطول الموجي ٣٥٠ نانومتر و ٤١٠ نانومتر على التوالي. كذلك اظهرت العينات استجابة و كشف و كفاءة عالية عند تسليط فرق جهد و كثافة قدرة قليلة. تم حساب تيار-فولتية عند اطوال موجية مختلفة من مصدر ضوئي زئبقي.

Introduction

Among various one-dimensional metal oxide nanostructures, zinc oxide (ZnO) has become the most important material to fabricate the UV-photodetector devices because of its unique physical and chemical properties, high electron mobility, wide bandgap (3.37 eV), large binding energy (~ 60 meV), and environmentally friendly semiconductor [1, 2]. There are various growth techniques to fabricate ZnO nanostructures, such as pulsed laser deposition [3], sol gel process [4], molecular beam epitaxy [5], and electrospinning technique [6].

Among those, the electrospinning was a controllable, simple, and low cost method to fabricate one dimensional ZnO nanostructures. However, efficiency of one dimensional ZnO nanostructures based UV-photodetector depends on wavelength, selectivity, illumination intensity, and bias voltage [7].

One dimensional ZnO nanostructures based UV-photodetector can be significantly improved by combining with other metal oxides such as (Co, MgO, Cu) which are more sensitive than pure zinc oxide [8]. Copper oxide is a kind of p-type direct bandgap with a narrow bandgap (~1.5 eV). It displays a wealth of interesting properties such as non-toxic,

electrochemical activity, chemical stability, and it can be prepared by low cost solution methods [9].

In this work, we fabricate the ZnO-CuO nanofiber heterostructures by combining electrospinning and dip coating methods. The structural, optical, I-V characteristics are measured. To further study the responsivity, selectivity, detectivity, and quantum efficiency were analysis.

Chemicals

Zinc acetate dihydrate ((Zn $(CH_3COO)_2.2H_2O$), Scharlau, Spain), ethanol (C_2H_6O, Netherlands), Polyvinylpyrrolidone (PVP, MW=1,300,000, Sigma Aldrich, USA), Copper nitrate trihydrate ($Cu(NO_3)2.3H_2O$, BDH), Hexamethylenetetramine ($C_6H_{12}N_4$, BDH) were all used as received. Distilled water was used throughout the experiments.

2. Experimental part

2.1. Preparation of ZnO nanofiber

To fabricate ZnO nanofibers, electrospinning process was adopted figure (1). Polyvinylpyrrolidone (PVP) and Zinc acetate were used as precursor materials. Zinc acetate precursor was prepared by dissolving 40 wt.% in distilled water. Also, the PVP solution was prepared by dissolving 6 wt.% in ethanol. Both solutions were stirred for 1 hour at room temperature separately. Then, 7.5 wt.% of Zinc acetate solution was added to PVP solution with constant stirring for 2 hours at room temperature. The mixed solution of zinc acetate and PVP was obtained.

The mixed solution of pvp/zinc acetate was loaded into a plastic syringe (5 ml) connected to stainless steel needle (21-gauge). The distance between the syringe needle and substrate collector was 20 cm with applied voltage=16kV and the feeding rate of the solution was adjusted to 1ml/h. The resulting ZnO nanofibers were then calcined at 500°C for 3 hours.

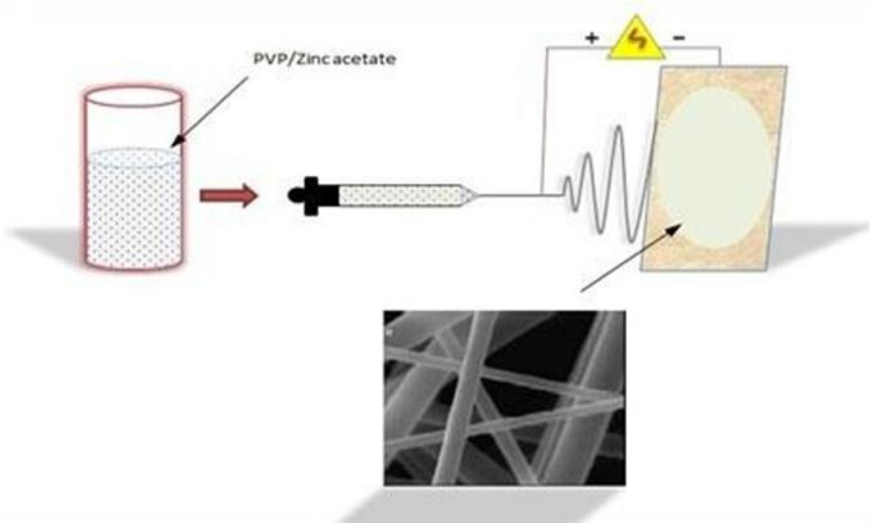

Fig.(1) Schematic view of electrospun pvp/zinc acetate nanofibers.

2.2. Preparation of ZnO-CuO nanofiber heterostructures

0.05 wt.% of copper nitrate trihydrate and 0.006 wt.% hexamethylenetetramine (HMT) was dissolved in 100 ml distilled water. ZnO nanofibers thin film was dipped in the above aqueous solution under slow stirring for 30 sec. Then, composite copper nitrate / ZnO nanofibers were annealing at 500 °C for 1 hour to transfer copper nitrate to CuO through thermal oxidation and obtained ZnO-CuO nanofiber heterostructures.

3. Characterization

The prepared ZnO-CuO nanofiber heterostructure was characterized by X-ray diffraction (XRD), field emission scanning electron microscope (FESEM). Also, UV-visible measurement of ZnO-CuO nanofiber heterostructures was recorded.

The photoelectric measurement of ZnO-CuO nanofiber heterostructures were studied under different power densities (1, 3, and 6 $\mu W/cm^2$) using mercury (Hg) lamp. Monochromator was used to exposed light at specific

wavelength to the sample. Also, current-voltage (I-V) measurements performed using Keithly-2430 digital electrometer and dual Farnel LT30/2 -3 to 3V power supply were used.

Results and discussions

Figure (2) (a, and b) shows the XRD patterns of ZnO nanofibers prepared by electrospinning technique and ZnO-CuO nanofiber heterostructures, respectively. The peaks shown in the XRD patterns corresponds to (100), (002), (101), (102), (110), and (103) Miller indices, reveal the formation of hexagonal wurtzite ZnO phase (JCPDS 36-1451). In ZnO-CuO nanofiber heterostructures just one more peak appears in (112) plane also indexed to monoclinic CuO JCPDS (05-0661). It could be observed that the CuO diffraction peaks are strong, implying to a large amount of CuO nanoparticles grown onto the ZnO nanofibers. Crystallite sizes were calculated from Scherrer's formula [10] : $D=k\lambda/(\beta\cos\theta)$ where, D is the average crystallite size, k a constant (=0.9 assuming that the particles are spherical), λ is the X-ray wavelength 0.15406 nm, θ is the Bragg diffraction angle and β is the full width at half maximum. The average crystallite size for ZnO nanofiber increased after dip-coating method from 16.26 to 24.07 nm. This increasing in crystallite size is due to the aggregation of each nanoparticle in ZnO nanofibers after dip- coating and annealing process. Also, the average crystallite size is 19.83 nm for CuO in ZnO-CuO nanofiber heterostructures.

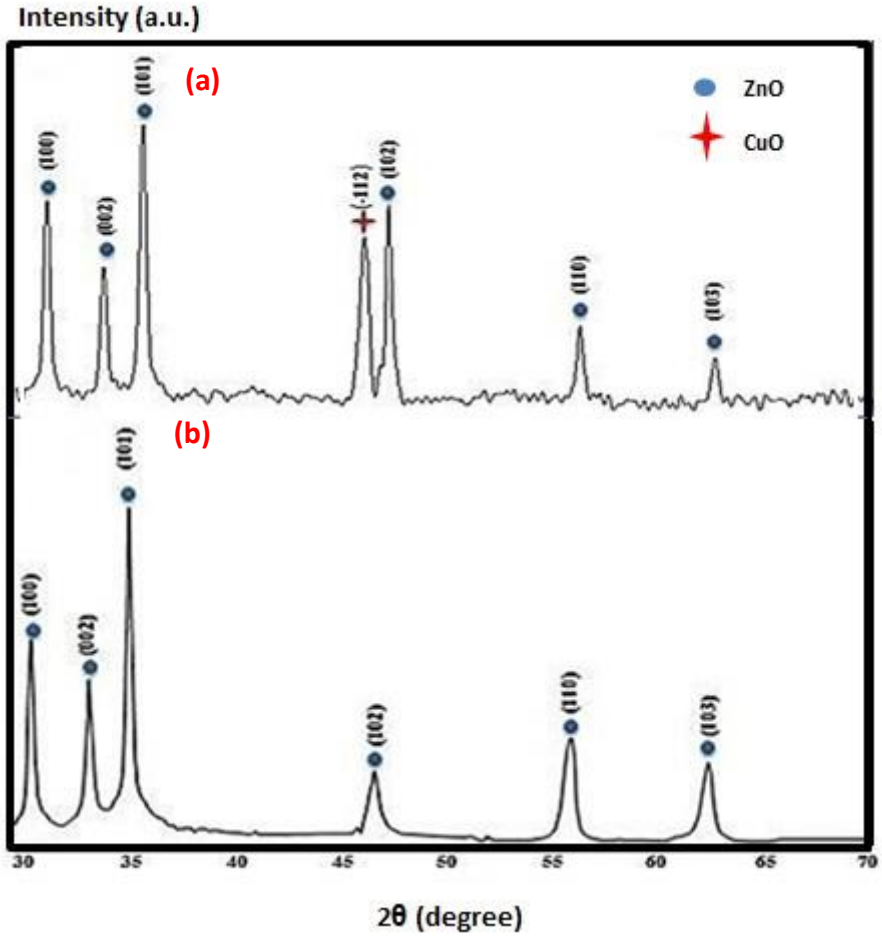

Fig.(2) XRD spectra of (a) ZnO nanofiber and (b) ZnO-CuO nanofiber heterostructures

The morphology of ZnO nanofiber and ZnO-CuO nanofiber heterostructures synthesized by combining electrospinning and dip coating methods are shown in figure (3). Figure (3a) shows that the average diameter for composite zinc acetate/pvp fiber is 228 nm before calcination process, and fibers have smooth surface and there are longer than several micrometers, therefore the aspect ratio is too high. After calcination process, the average diameter is decreased to 74 nm due to the calcination of organic PVP and the evaporation of water as shown in figure (3b). From figure (3c) it can be indicating that the surface of the ZnO nanofibers is covered by CuO nanoparticles which formed ZnO-CuO nanofiber

heterostructures and certainly increased the aspect ratio. Also, in ZnO-CuO nanostructures heterostructures the average particle size for ZnO is about 103 nm and the average particle size for CuO is about 39 nm.

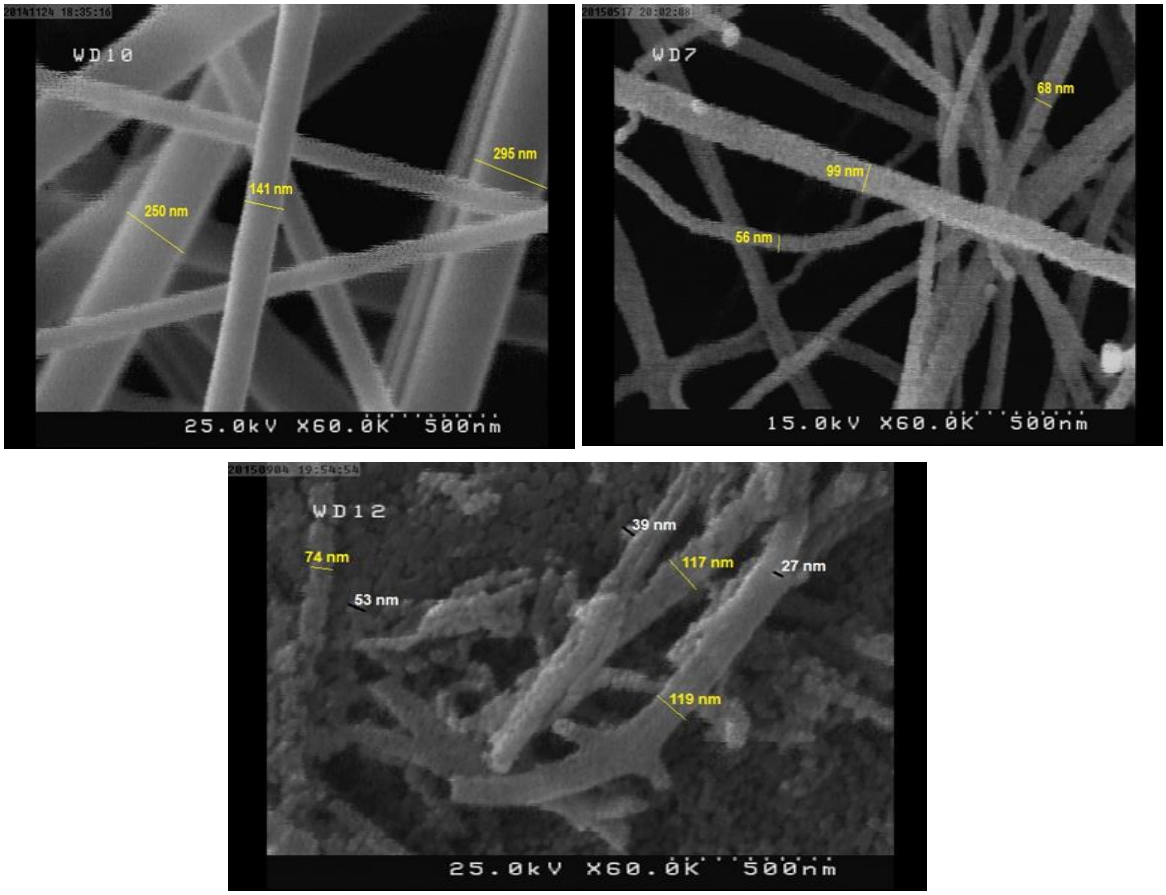

Fig.(3) FESEM images of: (a) Zinc acetate/pvp composite, (b) ZnO nanofibers , and (c) ZnO-CuO nanofiber heterostructures.

Figure (4a) shows the optical transmittance spectra of the ZnO nanofibers prepared by electrospinning technique. This figure shows low transmittance and higher energy than the energy gap of ZnO semiconductor in the (UV-VIS) range, which is 3.37eV. The bandgap of ZnO nanofibers is 3.67 eV as shown in figure (4b). This increasing in bandgap is due to confinement of material to nanometer scale. Figure (4c) shows that there is low transmittance below 400 nm attributed to small bandgap of CuO

nanoparticles (1.5 eV) that grown on the ZnO nanofibers. The effect of particle size is observed on the transmittance value, which is consistent with XRD results. The energy bandgap for ZnO-CuO nanofiber heterostructures is shown in figure (4d). The bandgap decreased compared to ZnO nanofiber from 3.67 to 2.95 eV after dip coating method, implying to decorating CuO nanoparticles on the surface of ZnO nanofibers as observed in FESEM results.

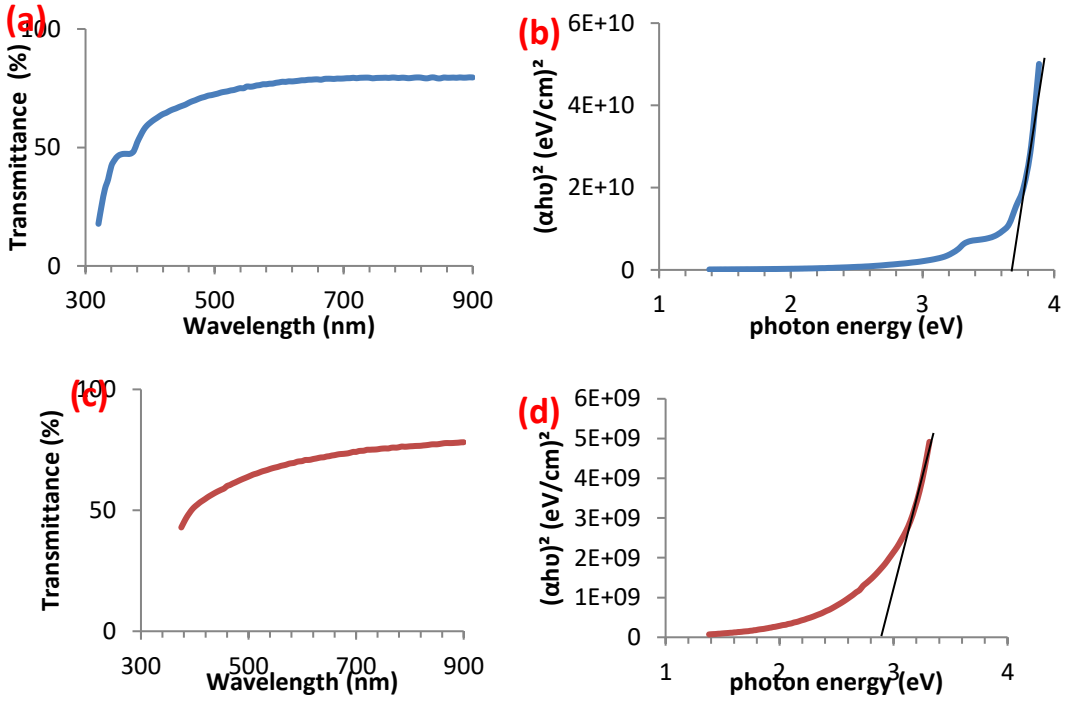

Fig. (4). Transmittance curves for (a) ZnO nanofiber and (c) ZnO-CuO nanofiber heterostructure, $(\alpha h\nu)^2$ vs. photon energy for (b) ZnO nanofiber and (d) ZnO-CuO nanofiber heterostructures.

The changing in resistance with illumination light of ZnO nanofiber and ZnO-CuO nanofiber heterostructures will study. ZnO nanofibers and ZnO-CuO nanofiber heterostructures were examined at different wavelengths from (300-600) nm and showed high response when illuminated with UV light (350 nm) and (410 nm) from mercury source for 40 second, respectively. As shown in figures (5) (a, and b) the resistance decrease very

fast suggesting increasing in surface conductivity of the specimen. However, it's clear that the specimen resistance dropped down about (44%) and (57%) for ZnO nanofiber and ZnO-CuO nanofiber heterostructures after illumination light, respectively. Compared to pure ZnO nanofibers, this more dropping in resistance in ZnO-CuO nanofiber heterostructures can attribute to the CuO nanoparticles that decorated on the surface of the ZnO nanofibers which increase the aspect surface to volume ratio and also p-n junction formation.

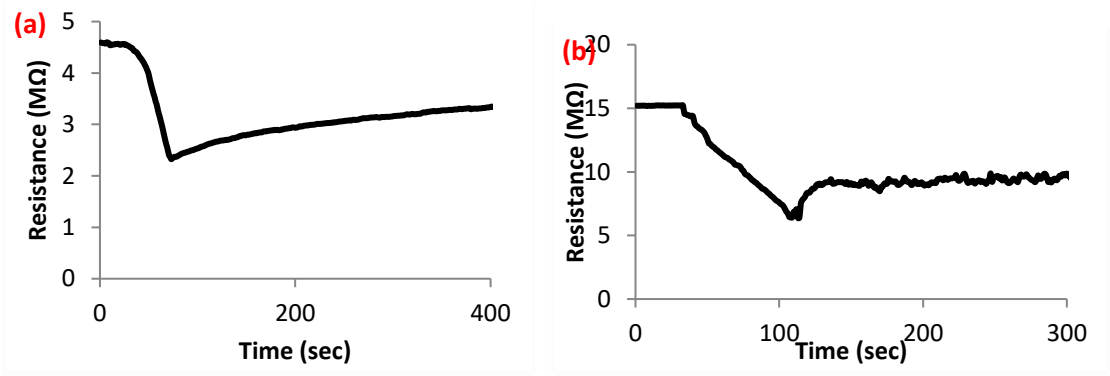

Fig.(5) Variation of resistance of (a) ZnO nanofibers, and (b) ZnO-CuO nanofiber heterostructure.

Figure (6) and (7) shows the current response of ZnO nanofiber and ZnO-CuO nanofiber heterostructures under different UV illumination, bias voltage, and power density (1.12, 3.38, 6.14 $\mu W/cm^2$), respectively. It's clear from these figures that the specimens show high spectral selectivity, where the high spectral response is at 350 nm for ZnO nanofiber and 410 nm for ZnO-CuO nanofiber heterostructures. Also, the current of the specimen increased with increasing the bias voltage and power density.

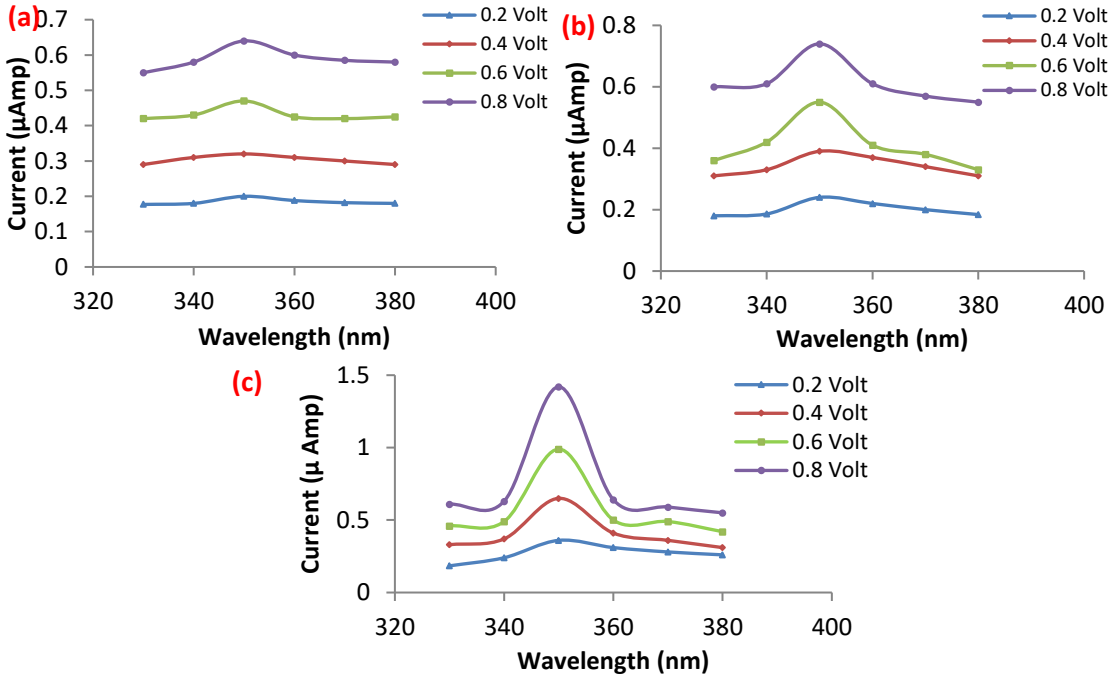

Fig. (6) Variation of current with illumination wavelength at different applied voltage for ZnO nanofibers at power densities: (a) 1.12 µW/cm^2, (b) 3.38 µW/cm^2, and (c) 6.14 µW/cm^2.

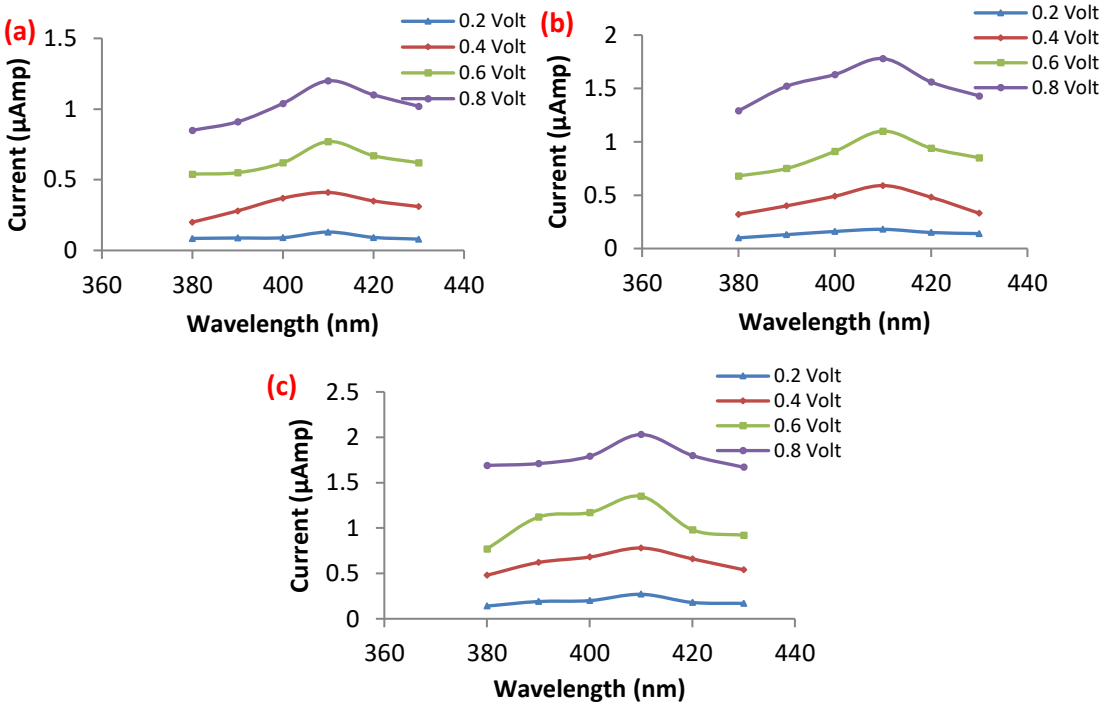

Fig.(7) Variation of current with wavelength at different applied voltage for ZnO-CuO nanofiber heterostructures at power densities: (a) 1.12 µW/cm^2, (b) 3.38 µW/cm^2, (c) 6.14µW/cm^2.

The dependence of current on the applied voltage (I-V) characteristic are shown in figures (8) (a, and b) for ZnO nanofiber and ZnO-CuO nanofiber heterostructures, respectively. The (I-V) characteristics were examined for different power densities by changing bias voltages (0.2, 0.4, 0.6, and 0.8 volt) at illumination wavelength (350 nm) and (410 nm) for ZnO nanofiber and ZnO-CuO nanofiber heterostructures, respectively.

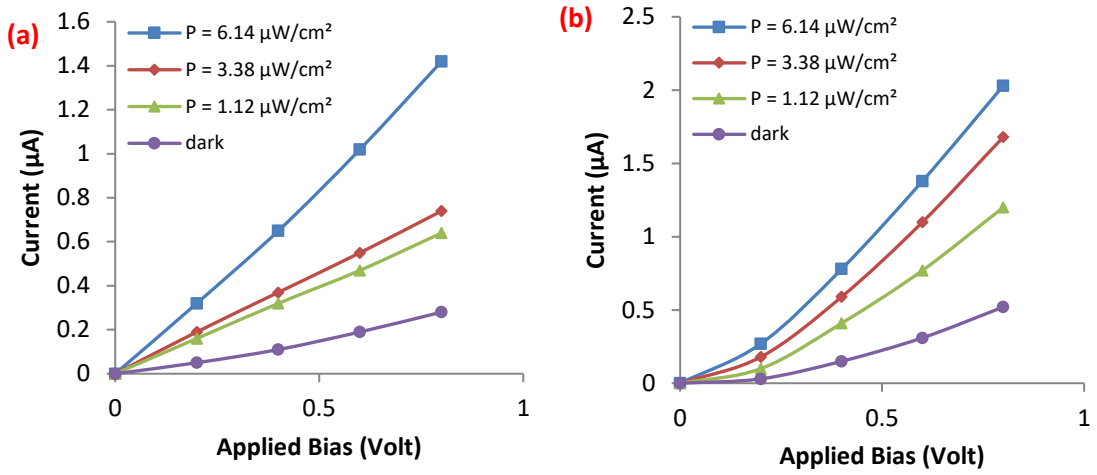

Fig.(8) (I-V) characteristic at illumination wavelength(a) (350 nm) for ZnO nanofibers, and (b) (410 nm) for ZnO-CuO nanofiber heterostructures.

The responsivity, detectivity, and the quantum efficiency of ZnO nanofibers and ZnO-CuO nanofiber heterostructures were calculated and found to be (0.1856 A/W), (9.7× 10^{11} cm.$Hz^{1/2}$.w^{-1}), and (0.00065) for ZnO nanofiber and (0.2850 A/W), (11× 10^{11} cm.$Hz^{1/2}$.w^{-1}), and (0.00086) for ZnO-CuO nanofiber heterostructures, respectively. The photodetector responsivity R_λ is calculated by:

$$\mathbf{R_\lambda = \frac{I - I_{dark}}{P_\lambda}}$$

Where P_λ is incident power, I is photo-current, and I_{dark} is dark current. Also, the detectivity (D*) can be calculated by the following expression:

$$\mathbf{D^* = \frac{R_\lambda}{\sqrt{2qI_{dark}}}}$$

Where q is electron charge. The quantum efficiency η was calculated using the following equation:

$$\eta = \mathbf{1.24}\ \frac{R_\lambda}{\lambda}$$

where λ is illumination wavelength.

Conclusion:

In summary, ZnO nanofibers prepared by electrospinning technique and ZnO-CuO nanofiber heterostructures were prepared by combining electrospinning and dip coating methods. ZnO-CuO nanofiber heterostructures showed fast response, high responsivity, detectivity, and efficiency than pure ZnO nanofibers and that can attribute to the CuO nanoparticles that decorated on the surface of the ZnO nanofibers which increase the aspect surface to volume ratio also p-n junction formed.

References:

[1] Liu C. Y., Zhang B.P., Lu Z.W., Binh N. T., Wakatsuki K., Segawa Y., Mu R., "fabrication and characterization of ZnO film based UV photodetector", journal of material science:Mater electron, Vol. 20, p 197-201, 2009.
[2] Jin Y., Wang Y., Sun B., Blakesley J. C., Greenham N. C., "Solution processed ultraviolet photodetectors based on colloidal ZnO", nanoparticles, Vol. 8, p 1649-1653, 2008.
[3] Vispute R. D., Talyansky V., Choopun S., Sharma R. P., Venkatesan T., He M., Tang X., Halpern J. B., Spencer M. G., Li Y. X., Jones K. A., " Pulsed laser deposition and processing of wide bandgap semiconductors and related materials", Applied Physics Letter, Vol. 28, p 275–286, 1999.
[4] Prakash G. S., "Synthesis and characterization of Zinc Oxide nanoparticles by sol – gel process", National institute of technology, Rourkela, 2012.
[5] Wang S. P., Shan C. X., Yao B., Li B. H., Zhang J. Y., Zhao D. X, Shen D. Z., Fan X. W., "Electrical and optical properties of ZnO films grown by molecular beam epitaxy", Applied Surface Science, Vol. 255, p 4913-4915, 2009.
[6] Raad S. Sabry, Firas S. Mohammed, Roonak Abdul Salam A.Alkareem, " Fabrication of electro spinning 1D ZnO Nano fibers as UV-Photoconductor", The 5th International scientific Conference on Nanotechnology& Advanced Materials Their Applications (ICNAMA 2015)3-4 Nov, 2015.
[7] Zhang Z., Kang Z., Liao Q., Zhang X., Zhang Y., " One-dimensional ZnO nanostructure-based optoelectronics", Chinese Physics B, Vol. 26, p 11, 2017.
[8] Suttinart N., Orathai T., Ki-S. A., "UV-Photodetectors based on CuO/ZnO nanocomposites", Materials Letters, Vol. 233, p 318-323, 2018.
[9] Moura A. P., Cavalcante L. S., Sczancoski J. C., Strppa D. J., Paris E. C., Ramirez A. J., Varela J. A., Longo E., "Structure and growth mechanism of CuO plates obtained by microwave-hydrothermal without surfactants", Advanced Powder Techniques, Vol.21, p 197-202, 2010.
[10] Kumar V., Dwivedi D. K., Agrawal P., "Optical, Structural and Electrical Properties of Nanosized Zinc Oxide Sintered Films for Photovoltaic Applications", Science of Sintering, 45: p. 13-19, 2013.